euspen's 22nd International Conference & Exhibition, Geneva, CH, May/June 2022
www.euspen.eu

A system calibration method for an embedded fringe projection system in a commercial electron beam powder bed fusion additive manufacturing machine (EBAM)

Yue Liu [1*], Liam Blunt[1], Feng Gao[1], Xiangqian Jiang[1]

[1]*EPSRC Future Metrology Hub, University of Huddersfield UK*

dryueyue1221@gmail.com

Abstract
Additive manufacturing (AM) processing technique can rapidly and efficiently fabricate three-dimensional (3D) parts of complex shapes and intricate structures that is not achievable using traditional methods, especially for metal AM by fusing metal powder in a layer-by-layer fashion. In these powder fusion machines, an in-situ inspection system to monitor the printed surface and preprint powder bed as the build cycle proceeds is important. Fringe projection profilometry is well-known for its ability to provide fast, high-precision, and full-field 3D measurement of objects in a non-contact manner. The implementation of a fringe projection system requires that the system is pre-calibrated to obtain high measurement precision and repeatability. This paper presents two calibration methods for an AM-based in-situ fringe projection system using a polynomial calibration. A circle ring board and a blank board are used during the system calibration. In addition to obtain good depth calibration results, more accurate transverse calibration results can be obtained. The proposed calibration methods to reduce the texture effect in the process of calibration is outlined. Experimental results show that the proposed methods can improve measurement precision and repeatability. The proposed in-situ/in-process inspection system has been implemented within a commercial electron beam powder bed fusion additive manufacturing machine (EBAM), to demonstrate the capability for effective feedback during the manufacturing process.

Keywords: system calibration; fringe projection; additive manufacturing

1. Introduction

Additive manufacturing (AM) techniques have been developing in recent years. As AM has a strong manufacturing ability to provide new solutions, especially for the building of complex geometries with internal structures, it has significant potential and space for development [1]. For any manufacturing technology, in-situ/online metrology is an effective supervision approach that can provide timely feedback to the process, thus improving the manufacturing efficiency. In AM processing, fringe projection systems are commonly used for in-situ detection methods. Fringe projection technology can provide a full-field, fast, high-resolution, and high-precision layer by layer areal surface measurement. Therefore, assessment of manufacturing quality would be advantageous in the process and provide feedback for process control[2].

A significant step for a fringe projection system is system calibration. System calibration is a process of determining the geometrical relationship between a camera and a projector, as well as the relationship between the world coordinate and the camera image coordinate, which affects the measurement resolution and repeatability. System calibration can be divided into camera calibration and geometric calibration. Existing geometric calibration methods for 3D inspection systems can be categorized into model-based [3], polynomial [4], and least-squares [5].

The Model-based method [6] is based on a geometrical model. The geometrical relationship between the camera and the projector is established by triangulation theory. After calculating system parameters, 3D data can be obtained by the phase information. The Least-squares method seeks to find the nonlinear relationship between the phase information and the 3D data. In this case, the calibration procedure becomes more flexible and easier, because system geometric parameters do not need to be calculated directly. The polynomial method seeks to express the relationship between the phase and depth coordinates by a polynomial relation, and the relation fits the relative position between the camera and the projector. Since the phase and depth relationship of the fringe projection system is close to linear, but due to nonlinear effects, lens distortion and other factors, more than three polynomials are needed to ensure the measurement repeatability.

In the calibration process, calibration boards with different calibrated marks are often employed, such as chess marks, ring marks, or circle marks. However, the colour of the marks affect the phase information recorded which causes phase error in the calibration process. In this paper, two system calibration methods are introduced. Two methods to address this so called "marks effect" to obtain high quality calibration results and to eliminate phase errors are proposed. One calibration method using a circle ring calibration plate, and the phase error caused by the rings is eliminated by using the fitting algorithm. This method eliminated the phase error in the circle rings region and reduced the random noise. The other method uses two calibration boards. One whiteboard is used to calibrate vertical direction, and the circle ring board is used to calibrate transverse direction. Experimental results show that both proposed methods eliminate the marks effect and improve measurement resolution and repeatability. The AM deployed fringe projection system has the capability to detect manufacturing defects,

which can improve manufacturing accuracy and control the process during the manufacturing. The developed system has been fully employed in a commercial AM machine and the associated control software.

2. Calibration Methods

The principle of the fringe projection technique is based on triangulation [7]. Based on triangulation principle, the geometric relationship of the projector and the camera can be represented by a mathematical relationship between the absolute phase map and depth data as follows

$$Z = \frac{L_0}{\frac{2\pi L_0^2 L\cos\theta}{P_0\Delta\varphi(x,y)(L_0+x\cos\theta\sin\theta)^2} - \frac{L\cos\theta\sin\theta}{L_0+x\cos\theta\sin\theta}+1} \quad (1)$$

It is difficult to directly obtain the system parameters L, L0, P0 for depth calibration (Equation 1). However, by using a Taylor series expansion, Equation 1 can be transformed into a polynomial function.

$$Z_r(x,y) = \sum_{n=0}^{N} a_n(x,y)\Delta\varphi(x,y)^n \quad (2)$$

where a_n, a_{n-1}, a_2, a_1 are sets of coefficients containing the depth parameters. n equals 5. The main task of calibration becomes the optimization of the coefficients of Equation 2. A reference surface is set in a reference coordinate system. Z_r is measurement height in reference coordinate system. Δϕ is the absolute unwrapped phase difference between the measured surface and the reference surface. The coefficients will have different values for every pixel and can be stored in a look-up table (LUT). If the phase information and the corresponding height information are known, the polynomial coefficients can be determined.

The relationship between transverse direction and depth direction is linear in thetically. However, there is a nonlinear effect because of the distortion of the optical lens.

Therefore, the relationship between X and Z, Y and Z can be expressed as quadric functions,

$$X_r(x,y) = b_1 Z_r(x,y)^2 + b_2 Z_r(x,y) + b_3 \quad (3)$$

$$Y_r(x,y) = c_1 Z_r(x,y)^2 + c_2 Z_r(x,y) + c_3 \quad (4)$$

where b_1, b_1, b_2, c_1, c_2, c_3 are the coefficients of the quadric in the reference coordinate system.

2.1. Fitting surface calibration

The calibration method needs two parts, depth calibration, and transverse calibration. In the depth calibration, a white ceramic diffuse plate with certified concentric circles markings is employed in the calibration procedure as shown in Figure 1. The circle board was accompanied by a calibration certificate guaranteeing the tolerance range of the centre positions within +/-0.002mm. An independent absolute distance measurement interferometer (Renishaw Model: ML10) is used in the calibration process. The circle ring board is placed on a transfer stage and moved to a series of positions in the measurement range. Based on the position of the calibration board, the middle position is taken as a reference surface. Based on the reference surface, a reference coordinate system (represents world coordinate system) can be constructed. At each position, the movement distance can be recorded by a length measurement traceable interferometer (as shown in Figure 1). At each position, the fringe patterns are projected onto the calibration board. The phase information from the projected fringe patterns of the calibration board is collected. After obtained phase data and depth data, a least-squares algorithm is employed to optimize the coefficient values based on Equation 2. Consequently, the geometric relationship between the camera and the projector can be determined.

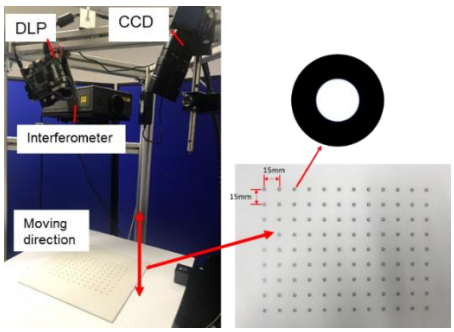

Figure 1 Fringe projection system and ceramic calibration board with concentric circles

Due to the presence of the black circle rings on the calibration board, the captured fringe patterns have low fringe contrast, which results in phase error and measurement error. A calibration approach based on a curve-fitting algorithm was applied to solve this problem. The modulation of the fringe patterns is calculated by Equation 5, which functions as a technique to remove the noisy points. By setting a threshold value, the outliers and the invalid points having low modulation can be identified.

$$M = \frac{2}{N}\times\sqrt{\left[\sum_{n=0}^{N-1} I_n \sin\left(\frac{2\pi n}{N}\right)^2\right] + \left[\sum_{n=0}^{N-1} I_n \cos\left(\frac{2\pi n}{N}\right)^2\right]} \quad (5)$$

M is the fringe modulation, N is phase-shifting steps, n is the captured image sequence, $\boldsymbol{I}_n$ is the intensity of the captured images. When M is under threshold value, the corresponding pixel will be set as invalid point. Therefore, the outliers crossing the circle ring area are removed, as shown in Figure 2. The unwrapped phase map is calculated from the rest of the wrapped phase data by using the optimum 3-frequency selection algorithm[8].

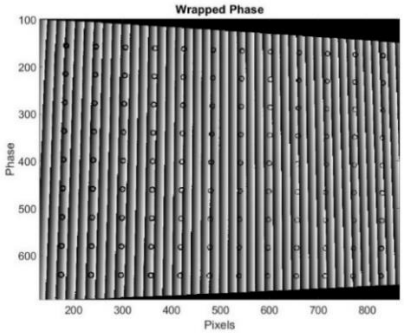

Figure 2. Wrapped phase map after identifying outliers

To fill in the invalid points, a quintic polynomial fitting equation was investigated to match the unwrapped phase data as Equation 6.

$$FittingPhase = P_0 + P_1x + P_2y + P_3x^2 + P_4xy + P_5y^2 + P_6x^3 + P_7x^2y + P_8xy^2 + P_9y^3 + P_{10}x^4 + P_{11}x^3y + P_{12}x^2y^2 + P_{13}xy^3 + P_{14}y^4 + P_{15}x^5 + P_{16}x^4y + P_{17}x^3y^2 + P_{18}x^2y^3 + P_{19}xy^4 + P_{20}y^5 \quad (6)$$

where x and y are the positions of the pixel, P_n is the coefficients of the fitting equation. Due to the fact that the calibration board is a flat white ceramic plate, the unwrapped phase map of the calibration board is ideally a plane. Theoretically, a linear fitting can determine the plane. Despite the effort of eliminating the distortion of the lens and the non-linearity of the system, the uneven fringe projection will still distort the unwrapped phase. Therefore, a relatively high-order fitting (quantic polynomial fitting) was used.

For transverse calibration, the camera captured texture images at each position. The phase maps and the corresponding marked points images are obtained. The height difference between the moving position of the circle ring board and the reference surface can be measured by the interferometer. The

coefficients of Equation 3 and Equation 4 are optimized by using the moving height results and the world coordinates of X and Y calculated by the centre point of the concentric circle as parameters. Consequently, the geometric relationship between the camera and the projector can be determined.

2.2. Whiteboard calibration

Another simple calibration method can also be used to solve this issue. It suits the system required high accuracy in the vertical direction and lower accuracy in the transverse direction. Figure 3 shows the procedure of the calibration method.

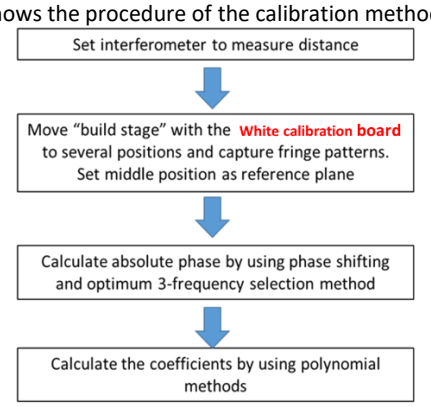

Figure 3. The procedure of the depth calibration

The calibration method needs two parts, depth calibration, and transverse calibration. In the depth calibration, a white flat calibration board is employed to obtain clear phase data.

The whiteboard is placed on the 'build stage' and moving to 21 positions. Based on the position of the calibration board, the middle position is as a reference surface. Based on the reference surface, a reference coordinate system (represents world coordinate system) can be constructed. Moving direction is the Z-axis. At each position, the movement distance can be measured by the interferometer. At each position, the fringe patterns are projected onto the white calibration board. The phase information from the projected fringe patterns of the calibration board is collected. After moved to 21 positions, 21 absolute phase maps can be obtained, and the corresponding moving distance measured by the interferometer. Based on these obtained phase data and depth data, a least-squares algorithm is applied to optimize the coefficient values of Equation 2. A set of high accuracy coefficients of Equation 2 can be calculated pixel by pixel, which results do not have the black ring effect.

After obtained the coefficients of Equation 2, the depth calibration is completed. The whiteboard is replaced by the circle ring board on the 'build stage' to do transverse calibration. The circle ring board is moved to 10 positions, which are in the field of calibrated depth. The same sinusoidal fringe patterns are projected on the circle ring board. The camera captured them and a texture image at each position. The height difference between the moving position of the circle ring board and the reference surface can be calculated by Equation 2. A crossline of the calculated height is selected where does not through the ring area, the selected height is fitted by the polynomial equation. The coefficients of Equation 3 and Equation 4 are optimized by using the fitting height results and the world coordinates of X and Y calculated by the centre point of the concentric circle same as method 2.1. Consequently, the geometric relationship between the camera and the projector can be determined.

3. System evaluation

In order to demonstrate the system performance, parameters including measurement, precision, repeatability reliability, and resolution (the minimum measurement depth), were evaluated.

3.1 Precision and resolution along transverse direction

During the calibration process, four test positions were recorded as known heights which are determined by the interferometer. Based on the four test positions, comparison with the nominal distance between each centre points and the measured distance is the transverse direction accuracy. Table 1 shows transverse calibration the results.

Table 1 Details of the accuracy and precision along transverse direction

Directions	Nominal distance between each centre points (mm)	Number of centre to centre measurements	Mean measured distance (mm)	Mean absolute errors (measurement accuracy) (mm)	Standard deviation (Precision) (Units: mm)
X	15.0007	320	15.0228	0.0228	0.0467
Y	15.0009	308	14.9971	0.0029	0.0382

The measurement accuracy and repeatability of x-direction are 0.0228mm and 0.0467mm respectively. The measurement accuracy and repeatability of y-direction are 0.0028mm and 0.0387mm respectively. The transverse resolution is defined as the ratio of the field of view and the resolution. The resolution of the used camera is 4016 by 3016. The Field of view is around 200mm by 180mm. Therefore, the transverse resolution is 0.050mm and 0.060mm in x and y directions, respectively. It can be clearly seen that the measurement accuracy in the Y direction is higher than that in the X direction because there was an angle between the optical axis of the camera and the normal line of the calibration plate when the camera operating. Because of the angle, a perfect circle becomes an ellipse in the camera view. The centre of the ellipse extracted in the X direction deviated from the true centre of the circle, while the deviation between the extracted centre of the ellipse and the true centre in the Y direction was small, so the accuracy in the Y direction is higher.

3.2 Precision and resolution along z direction

Table 2 Details of the accuracy and precision along depth direction

	Position (mm)	Mean measured distance	Mean absolute error (Measurement accuracy)	Standard deviation (precision)
Method 2.1	3.5011	3.4832	0.0179	0.0050
	1. 5030	1.5000	0.0030	0.0072
Method 2.2	-5.3987	-5.3728	0.0259	0.0168
	1.2982	1.2954	0.0028	0.0126

The height value of tested sample can be calculated based on Equation 2. During the calibration process, four testing positions were used as known heights determined by using the independent interferometer with two calibration methods. Based on the calibrated coefficients and the absolute phase, the measured height of the object can be acquired. System mean absolute error can be acquired by comparing the value measured from the interferometer with the height measured from the system. The measured distance obtained by the interferometer was taken as the ideal value. System repeatability and reliability can be evaluated by calculating the standard deviation. After compared with two methods, the measurement accuracy of two methods is close and both methods solved circle ring impact, the standard deviation of method one is smaller than method two. Table 2 shows the results. The EBM machine required 100 micrometers depth

resolution. Therefore, the fringe projection system meets the requirement.

4. Experiments

A conceptual illustration of the EBM machine setup with fringe projection system is shown in Figure 4. The AM machine consists of four parts with different functions: they are an electron beam melting source, a powder delivery system, a powder bed transfer stage, and the fringe projection inspection system. The final implementation is within a commercial EBM machine. The inside of machine chamber is under vacuum during the process. The fringe projection system is fixed on top of the machine. The fringe projection system consists of a CCD (charge-coupled device) camera and a DLP (digital light processing) projector. The camera and projector are located on either side of the electron beam melting source. The position of the projector and the camera are fixed with the angle between the optical axes of circa 30°. The inspected surface is at the intersection of the axes.

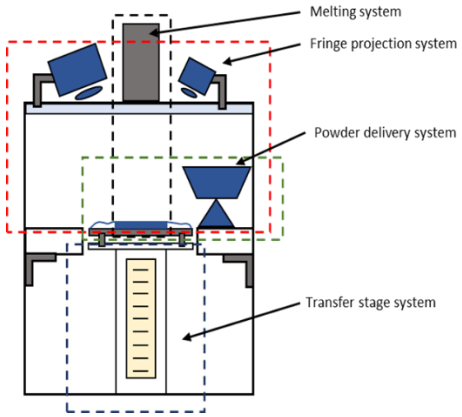

Figure 4. A conceptual set up of the fringe projection inspection system

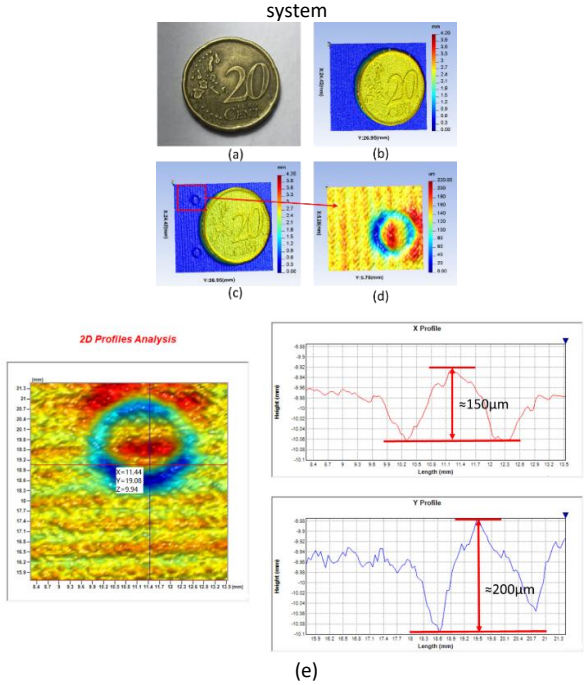

Figure 5. A twenty-cent coin and 3D reconstruction results. (a) Photograph of the coin; (b) 3D measurement results of the coin after corrections. (c) 3D measurement results of the coin before corrections (d) Zoom in the error (e) The 2D profile of the measurement error because of ring effect.

3D results of proof of concept measurement samples were shown in Figure 5 and Figure 6. Figure 5 was a 3D measurement result of a coin. Figure 5(a) shows a twenty-cent coin. Figure 5(b) shows the 3D measurement results of the coin after corrections by proposed method. Figure 5(c) shows the 3D measurement results of the coin before corrections. Figure 5 (d) was the zoomed error area of 3D measurement results. Figure 5 (e) was the 2D profile of the measurement error because of ring effect. The proposed calibration method clearly eliminated the effect of the rings.

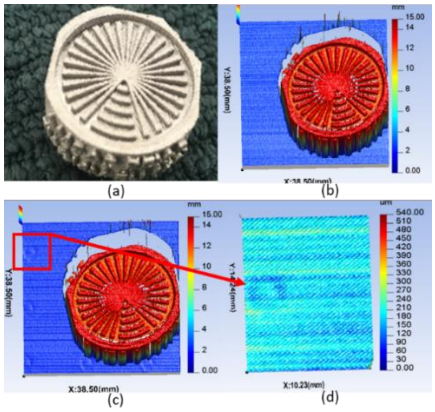

Figure 6. Printed metal sample and 3D reconstruction results. (a) Photograph of tested printed sample (b) Areal map of tested printed sample after corrections (c) Areal map of tested printed sample before corrections (d) Zoom in the error

An Ebeam AM printed metal sample was measured by the fringe projection system as shown in Figure 6(a). The printed metal part with radial grooves and ridges is used for evaluating the manufacturing resolution. The measured results were consistent with the manufacturing resolution. Comparing results with the proposed method and without corrections method, shows that the ring effect was eliminated, the measurement error of the rings area has been improved by 150 µm to 200 µm.

5. Conclusions

This paper presented two calibration methods for an AM-based in-situ fringe projection system using a polynomial calibration model. A circle ring board and a blank board are used during the system calibration. In addition to obtain good depth calibration results, more accurate transverse calibration results can be obtained. The proposed calibration method to reduce the texture effect in the process of calibration is outlined. Experimental results show that the proposed methods can improve measurement precision and repeatability. The proposed in-situ/in-process inspection system has been implemented within a commercial electron beam powder bed fusion additive manufacturing machine (EBAM), to demonstrate the capability for effective feedback during the manufacturing process.

References

[1] Liu Y, Blunt L, Zhang Z, Rahman H A, Gao F,Jiang X 2020 *J Addit Manuf.* Vlo **31**, Jan 2020 100940
[2] Liu Y, Blunt L, Gao F, Jiang XJ 2021 Jun *Surface Topography: Metrology and Properties* **17**
[3] Zhang Z, Zhang D, Peng X 2004 Sep 1 *Optics and lasers in engineering* **42**(3):341-53
[4] Jia P, Kofman J, English CE 2007 Apr *Optical Engineering* **46**(4):043601
[5] Huang L, Chua PS, Asundi A 2010 Mar 20 *Applied optics* **49**(9):1539-48
[6] Hu Q; Huang PS; Fu Q; Chiang FP 2003 Feb *Optical Engineering*
[7] Zhang Z, Zhang D, Peng X 2004 Sep 1 *Optics and lasers in engineering* **42**(3):341-53
[8] Towers CE, Towers DP, Jones JD 2005 Jul 1 *Optics and Lasers in Engineering* **43**(7):788-800